

Folliculostellate cell network: A route for long-distance communication in the anterior pituitary

Teddy Fauquier*, Nathalie C. Guérineau*, R. Anne McKinney†, Karl Bauer‡, and Patrice Mollard*§

*Institut National de la Santé et de la Recherche Médicale (INSERM) Unité 469, Centre National de la Recherche Scientifique–INSERM de Pharmacologie–Endocrinologie, 141 Rue de la Cardonille, 34094 Montpellier Cedex 5, France; †Brain Research Institute, University of Zurich, Winterthurerstrasse 190, CH-8057 Zurich, Switzerland; and ‡Max-Planck-Institut für Experimentelle Endocrinologie, Feodor-Lynen-Strasse 7, 30625 Hannover, Germany

Edited by Michael V. L. Bennett, Albert Einstein College of Medicine, Bronx, NY, and approved May 9, 2001 (received for review July 21, 2000)

All higher life forms critically depend on hormones being rhythmically released by the anterior pituitary. The proper functioning of this master gland is dynamically controlled by a complex set of regulatory mechanisms that ultimately determine the fine tuning of the excitable endocrine cells, all of them heterogeneously distributed throughout the gland. Here, we provide evidence for an intrapituitary communication system by which information is transferred via the network of nonendocrine folliculostellate (FS) cells. Local electrical stimulation of FS cells in acute pituitary slices triggered cytosolic calcium waves, which propagated to other FS cells by signaling through gap junctions. Calcium wave initiation was because of the membrane excitability of FS cells, hitherto classified as silent cells. FS cell coupling could relay information between opposite regions of the gland. Because FS cells respond to central and peripheral stimuli and dialogue with endocrine cells, the form of large-scale intrapituitary communication described here may provide an efficient mechanism that orchestrates anterior pituitary functioning in response to physiological needs.

Classically, the anterior pituitary is considered as a secondary oscillator obeying mainly hypothalamic factors, either increasing or decreasing secretion of pituitary hormones, which are released in an episodic manner at the base of the median eminence (1–4). The portal blood vessels form the interorgan communication system driving the hypothalamic inputs to the anterior pituitary. They collect the transmitters released by hypothalamic nerve endings at the primary capillary plexus level and slowly distribute them in the endocrine parenchyma via the arborescence of pituitary sinusoids between the columnar units of pituitary cells (“cell cords”) (5, 6). Over the last three decades, many studies carried out in isolated endocrine cells have provided strong evidence that endocrine cells generate action potential-driven rises in cytosolic Ca^{2+} concentration ($[\text{Ca}^{2+}]_i$) that are probably the keystones of dynamic adjustment of numerous cellular functions, including exocytosis and gene expression (7–9). Recently, the technique of acute slice preparations applied to the anterior pituitary revealed that endocrine cells do fire short-term $[\text{Ca}^{2+}]_i$ transients because of their electrical activity *in situ* (10, 11).

However, the activity of the gland as a whole does not reflect the average of independent dynamics of cellular messages that occur in the distinct endocrine cell types scattered throughout the tissue. In this respect, one puzzling finding is the persistence of pulsatile releasing profiles of hormones when the gland is disconnected from the hypothalamic inputs (12, 13). This indicates that a large-scale communication system exists *within* the anterior pituitary. Despite the wealth of information on cell-to-cell mechanisms between endocrine cells that comprise the release of paracrine factors (14) and gap junction signaling (10), spreading of spatial information that crosses the limits of single cell cords could not be explained by these mechanisms.

Because a highly efficient process spreading spatial information to the entire gland and even to pituitary subregions has not been reported yet, we explored here whether nonendocrine folliculostellate (FS) cells can support long-distance information

transfer within the gland. FS cells display a star-shaped cytoplasmic configuration intermingled between hormone-secreting cells. The organization of FS cells within the parenchyma forms a three-dimensional anatomical network, in the meshes of which the endocrine cells reside (15, 16). Very little is known about the functioning of this FS cell network, in particular with regard to the dynamics of cellular/intercellular messages. To study the behavior of this network, we measured multicellular changes in $[\text{Ca}^{2+}]_i$, a messenger involved in a wide range of cell-to-cell communication mechanisms (17–23), electrophysiological properties of FS cells, and intercellular diffusion of dyes in acute pituitary slices. We show here that the FS cell network forms a functional intrapituitary circuitry in which information— Ca^{2+} signals and small diffusible molecules—can be transferred over long distances (millimeter range) within the intact pituitary tissue.

Methods

Cytosolic Ca^{2+} Monitoring in Acute Slices. Pituitary slices (200 μm thick) from 10- to 12-week-old female Wistar rats were prepared as previously described (11). Ringer’s saline contained (in mM): 125 NaCl/2.5 KCl/2 CaCl₂/1 MgCl₂/1.25 NaH₂PO₄/26 NaHCO₃/12 glucose. Slices were incubated with 40 μM β -Ala-Lys-*N*^ε-AMCA, a UV light-excitabile fluorescent dipeptide (AMCA, 7-amino-4-methylcoumarin-3-acetic acid) taken up by FS cells (24), at 37°C for 1.5 h and then exposed to 15 μM Oregon green 488 1,2-bis(2-aminophenoxy)ethane-*N,N,N',N'*-tetraacetate (BAPTA)-1 acetoxymethyl ester (Molecular Probes) periodically delivered (3 s per 20 s for 15–20 min) onto a cell field via a blunt micropipette (11). Time-lapse optical sequences were captured with a real-time confocal microscope (Noran Odyssey XL, 488-nm excitation wavelength, 120 images per s with averaging 4 frames), which also delivered a TTL (transistor-transistor logic) signal that synchronized image acquisition with a brief voltage pulse (1 ms, 0.5–10 V) applied to a patch-pipette filled with Ringer’s saline and positioned on the cell (10). Because the confocal microscope was fitted with an Ar/Kr laser (visible light wavelengths), cells at the slice surface were first viewed with a xenon lamp via the epifluorescent port of the upright microscope. Only cells that showed both β -Ala-Lys-*N*^ε-AMCA and Oregon green 488 BAPTA-1 were taken for subsequent $[\text{Ca}^{2+}]_i$ monitoring. In some experiments, electrical field stimulation was used to locally stimulate a cell field. A current step was shortly applied between the tips (50–100 μm apart) of two pipettes (filled with Ringer’s saline) touching the slice

This paper was submitted directly (Track II) to the PNAS office.

Abbreviations: FS, folliculostellate; $[\text{Ca}^{2+}]_i$, cytosolic calcium concentration; TTX, tetrodotoxin; TEA, tetraethylammonium; BAPTA, 1,2-bis(2-aminophenoxy)ethane-*N,N,N',N'*-tetraacetate; AMCA, 7-amino-4-methylcoumarin-3-acetic acid; IP₃, inositol 1,4,5-trisphosphate.

§To whom reprint requests should be addressed. E-mail: mollard@u469.montp.inserm.fr.

The publication costs of this article were defrayed in part by page charge payment. This article must therefore be hereby marked “advertisement” in accordance with 18 U.S.C. §1734 solely to indicate this fact.

surface. $[Ca^{2+}]_i$ changes were imaged with an intensified cooled charge-coupled device camera (PentaMAX Gen IV; Princeton Instruments, Trenton, NJ) and acquired with Metafluor (Universal Imaging, Media, PA). Image analysis was carried out with INTERVISION 1.5.1, NIH IMAGE 68K 1.58, IGOR PRO 3.14, and ADOBE PHOTOSHOP 5.0. Pharmacological agents were either superfused or locally applied with a puff pipette.

Patch-Clamp Measurements. Whole-cell electrical events were recorded by using an EPC-9 patch-clamp amplifier (HEKA Electronics, Lambrecht/Pfalz, Germany). Intrapipette solution contained (in mM): 140 potassium gluconate/10 KCl/2 MgCl₂/1.1 EGTA/5 Hepes, pH 7.2 (KOH). Current steps were injected through the pipette tip at the soma level only. When membrane potential measurements were combined with $[Ca^{2+}]_i$ imaging, fluo-3 potassium salt (100 μ M) was included, and EGTA was lowered to 0.2 mM. Lucifer yellow (1 mM, Sigma) or Neurobiotin [*N*-(2-aminoethyl)biotinamide hydrochloride, 1%, Vector Laboratories] was added to the intrapipette solution when appropriate. When inward currents were recorded in voltage-clamp conditions, CsCl replaced potassium gluconate in equimolar amounts, and BAPTA (10 mM) was used as a Ca^{2+} chelator. Only cells with a high input resistance (≥ 1 G Ω), which provided acceptable space-clamp conditions, were recorded with the voltage-clamp mode.

Immunostaining. Laminin staining was performed with a polyclonal antibody (Sigma) when the FS cell network had been traced with Neurobiotin (revealed with FITC-labeled avidin D). Samples were examined with a Zeiss LSM 410 confocal microscope. Neurobiotin was visualized with an argon ion laser at 488 nm, and a He/Ne laser, pretuned to 543 nm, was used to image laminin simultaneously. Optical slices of 0.2- μ m intervals with each image averaged were used to improve the signal-to-noise ratio. Dual staining was reconstructed three-dimensionally by using Imaris software (Bitplane, Zurich).

Vaseline-Gap Technique. Coronal slices were placed in a two-compartment chamber so that the two slice sides were bathed in separate compartments. Insulation between compartments was secured by a thin Vaseline (petroleum jelly) bridge surrounding a slice portion of about 0.5 mm in width. One compartment was usually filled with β -Ala-Lys-*N*^e-AMCA-containing Ringer's saline, whereas the other contained peptide-free medium. Incubation for 3 h at 37°C was carried out to achieve intense AMCA fluorescence because of peptide uptake by FS cells. Fluorescent lectins were routinely included in the bathing solutions to check the water-tightness of the Vaseline bridge and to help delineate the bridge borders after slice fixation.

Results

Generation of Calcium Waves Within the FS Cell Network. Experiments were carried out in acute pituitary slices (10) to preserve the framework of the FS cell network. We visualized FS cells by incubating slices with β -Ala-Lys-*N*^e-AMCA, a fluorescent dipeptide that specifically accumulates in FS cells (24) (Fig. 1*a*). In addition, short-term (≤ 15 –20 min) exposure with Oregon green 488 BAPTA-1 acetoxymethyl ester (11) allowed Ca^{2+} dye loading of β -Ala-Lys-*N*^e-AMCA-positive FS cells before loading the neighboring endocrine cells to a detectable threshold (Fig. 1*b*). Voltage from a micropipette touching an FS cell was used to deliver local electrical stimulation (10), whereas multicellular $[Ca^{2+}]_i$ changes were monitored with real-time confocal microscopy. Brief stimulation triggered a fast-peaking $[Ca^{2+}]_i$ rise (time to peak < 1 s), which was conveyed from one FS cell to the next (Fig. 1*c*) (156 of 176 trials, 59 different slices). The apparent velocities of $[Ca^{2+}]_i$ waves (measured from the delays between onsets of $[Ca^{2+}]_i$ rises in FS cell somas located at the same optical

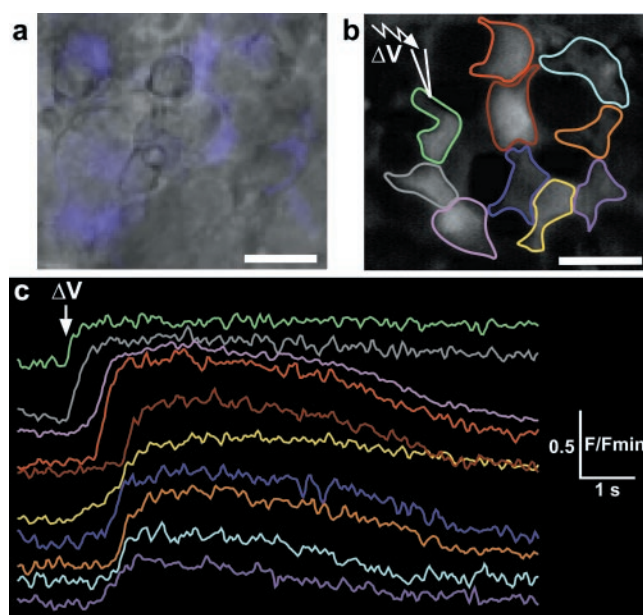


Fig. 1. Generation of propagated $[Ca^{2+}]_i$ waves in FS cells in response to electrical stimulation. (a) Superimposed differential interference contrast microscopy image of the slice surface with β -Ala-Lys-*N*^e-AMCA fluorescence (pseudocolored in blue) of FS cells (scale bar, 10 μ m). (b) A confocal image showing 10 FS cells loaded with a fluorescent Ca^{2+} dye (scale bar, 10 μ m). The color circles highlight the area of each cell used to monitor changes in fluorescence reflecting $[Ca^{2+}]_i$ levels. The stimulating micropipette was touching the cell circled in green. (c) Changes in fluorescence, normalized to baseline fluorescence (F/F_{min}), for the 10 regions in *b*. The spread of a $[Ca^{2+}]_i$ wave was initiated by a brief electrical stimulation. Onset of the stimulation is indicated by an arrow.

plane) were 124 ± 13 μ m/s ($n = 207$ cells, 23 fields). The $[Ca^{2+}]_i$ rises observed in FS cells distant from the site of stimulation resulted from propagated $[Ca^{2+}]_i$ waves. It is highly unlikely that these $[Ca^{2+}]_i$ rises were the result of direct electrical excitation as they did not occur simultaneously, but only when a stimulation was applied through a pipette in contact with an FS cell, and they did not spread uniformly in all directions. Finally, it should be noted that the FS cell network could also work as an autonomous system because $[Ca^{2+}]_i$ waves propagating spontaneously between FS cells at a single plane of focus were occasionally observed during long-lasting optical recordings and in the absence of any stimulation electrode (data not shown).

FS Cell Membrane Excitability Is Responsible for Initiating $[Ca^{2+}]_i$ Waves. Establishing $[Ca^{2+}]_i$ transients in FS cells mostly depends on membrane excitability because tetrodotoxin (TTX, 0.5 μ M), a specific Na^+ channel antagonist, reversibly blocked the $[Ca^{2+}]_i$ transients in FS cells that propagated $[Ca^{2+}]_i$ waves (Fig. 2*a*, 8 of 10 cell fields). Also, Cd^{2+} , a blocker of voltage-gated Ca^{2+} channel currents, completely suppressed both the initial $[Ca^{2+}]_i$ rise and propagated waves (7 of 7 cell fields, data not shown). This result was astonishing because FS cells were previously considered to be silent cells (25). We therefore examined the electrical membrane properties of FS cells with the whole-cell patch-clamp technique. FS cells showed a resting potential of -61 ± 5 mV ($n = 115$) and displayed a remarkably wide range of input resistance (35 M Ω to 4.2 G Ω), which occasionally varied during the time period of recordings. When FS cells had a relatively high input resistance (≥ 1 G Ω), action potentials could be triggered upon step depolarization in 37 of 70 of these cells (Fig. 2*b–d*). In the remainder cells recorded under current-clamp conditions, the spatiotemporal current flow along the

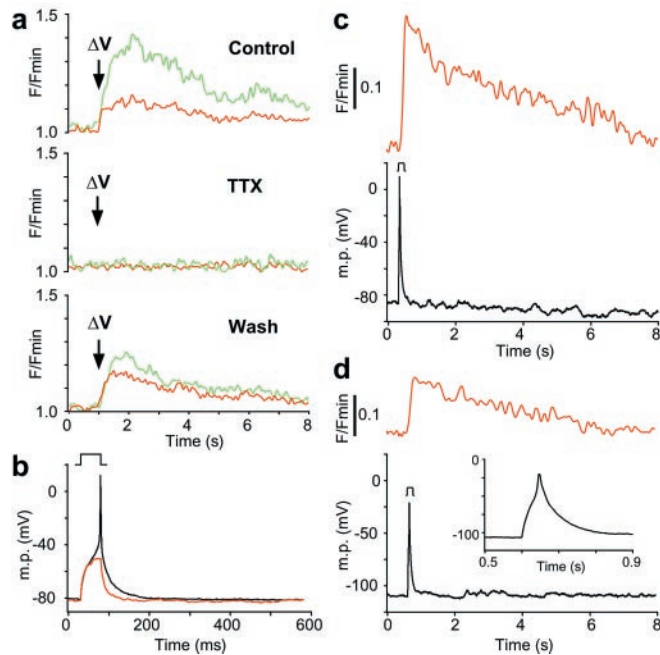


Fig. 2. Generation of $[Ca^{2+}]_i$ transients depends on membrane excitability. (a) Stimulated $[Ca^{2+}]_i$ transients in two adjoining FS cells (red trace: triggered cell) in normal Ringer's saline (Top) and in the presence of $0.5 \mu M$ TTX (Middle) are shown. (Bottom) The TTX-mediated alteration of $[Ca^{2+}]_i$ transients recovered after a 12-min wash. (b) Step current injection triggered an all-or-none action potential (black trace), which was suppressed in the presence of $0.5 \mu M$ TTX (red trace). (c) Current-clamp recording of a single action potential triggered upon current step (Lower) that caused a transient rise in $[Ca^{2+}]_i$ (Upper). (d) Similar combined electrical and optical recordings in a TTX-treated cell. (Inset) The TTX-resistant spike on expanded time scale.

processes might not have been strong enough to generate ectopic action potentials (23), as most FS cells emit prolonged cell processes with distal "end-feet" (16). TTX consistently suppressed the fast component of action potentials (Fig. 2*b*). Smaller spikes, however, were observed in some TTX-treated cells (Fig. 2*d*). Both types of action potential were able to induce a transient $[Ca^{2+}]_i$ rise when patch-clamp recordings were simultaneously combined with $[Ca^{2+}]_i$ imaging (Fig. 2*c* and *d*, 10 of 15 cells).

As the initiation of $[Ca^{2+}]_i$ waves most probably depended on action potential firing, we characterized the voltage-gated conductances expressed in FS cells. When K^+ currents were blocked by Cs^+ dialysis through the patch-clamp pipette, a fast-activating, fast-inactivating TTX-sensitive inward Na^+ current was measured in 27 of 43 cells (Fig. 3*a*). In 51 of 84 cells recorded in the presence of both TTX and Ba^{2+} ions, step depolarization triggered voltage-gated inward currents flowing through Ca^{2+} channels that were abolished by Cd^{2+} ions (Fig. 3*b*). It should be noted that the activation threshold of Ca^{2+} currents corresponded to the threshold of TTX-resistant spikes (Fig. 2*d*). Besides the voltage-dependent switch-off of both Na^+ and Ca^{2+} currents, spike repolarization probably involved K^+ currents in FS cells because Ba^{2+} ions, a strong K^+ channel blocker, markedly prolonged action potential duration (100 ± 4 ms calculated at 50% of spike repolarization, 4 of 9 cells, data not shown). In over 57 cells recorded in the presence of Ringer's saline, step depolarization could trigger at least two distinguishable outward currents, which both were most likely carried by K^+ ions (mean reversal potential: -74 ± 3 mV); 86% of cells showed a delayed outward K^+ current (mean activation threshold: -25 ± 0.3 mV) (Fig. 3*c*), which was suppressed by 15 mM

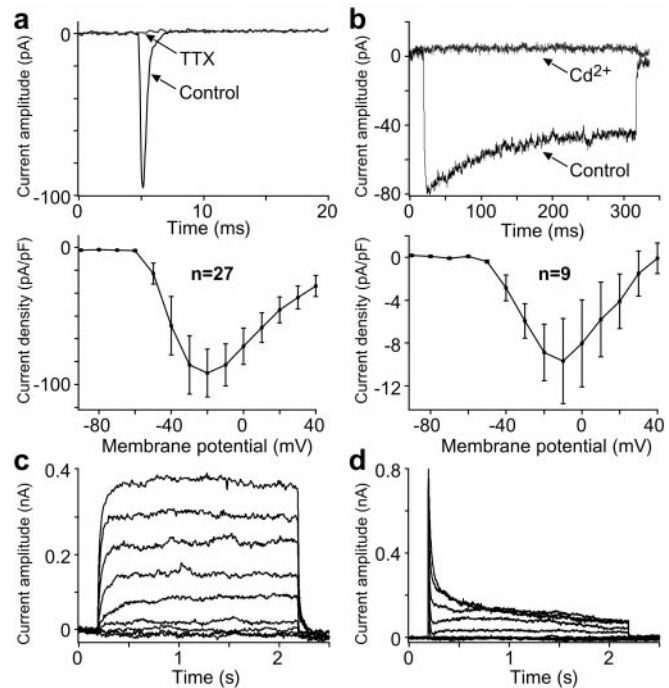


Fig. 3. Voltage-gated currents in FS cells. Voltage-clamp recordings were carried out in FS cells (holding potential = -80 mV). (a) Upper Inward current triggered upon step depolarization. TTX ($0.5 \mu M$) blocked the inward current. (Lower) Relative current-voltage relationship of the peak inward current (mean \pm SEM). (b) Upper Inward current carried by Ba^{2+} ions (in the presence of TTX) and triggered upon depolarization to -20 mV. Cd^{2+} ions ($500 \mu M$) suppressed the Ba^{2+} current. (Lower) Relative current-voltage relationship of peak Ba^{2+} current. (c) Outward currents triggered upon a series of voltage steps (-80 to $+80$ mV, 20-mV increment). (d) Similar recordings in another cell treated with 15 mM TEA.

tetraethylammonium ions (TEA, $n = 12$). In 70% of recorded cells, a transient outward K^+ current with a low threshold for voltage activation (-42 ± 0.3 mV) was observed. This transient current persisted in the presence of TEA (Fig. 3*d*), whereas it was reduced by more than 50% by 5 mM 4-aminopyridine ($n = 6$, data not shown).

$[Ca^{2+}]_i$ Wave Propagation Depends on Gap Junction Signaling. We

then explored the mechanism that underlies $[Ca^{2+}]_i$ wave propagation. Two sources of cell-to-cell communication not mutually exclusive could be involved. Gap junctions were observed along FS cell membranes (27, 28). FS cells are also known to release various products that may act on neighboring FS cells (14, 29).

We first examined whether the spreading of $[Ca^{2+}]_i$ waves required gap junction signaling. Carbenoxolone, a glycyrrhetic acid analog, reversibly reduced by $70.5 \pm 10\%$ the number of FS cells propagating $[Ca^{2+}]_i$ waves ($n = 10$ fields; $P < 0.001$, paired Student's two-tailed *t* test) (Fig. 4*a*). The action of carbenoxolone was most likely the result of its efficiency at blocking gap junctional communication (30) because (i) it did not alter the initial $[Ca^{2+}]_i$ rise in the stimulated FS cell (Fig. 4*a* Middle), (ii) it markedly decreased the cell-to-cell diffusion of small molecular weight dyes (Neurobiotin tracer, 13 fields; β -Ala-Lys- N^{ϵ} -AMCA, see below), (iii) it caused an increase in input resistance in FS cells probably reflecting a reduction of electrotonic coupling (841 ± 152 M Ω vs. $1,589 \pm 250$ M Ω in control and carbenoxolone-treated FS cells, respectively; $n = 41$ and 22, $P < 0.05$), and (iv) it also significantly diminished the propagation of intercellular $[Ca^{2+}]_i$ waves initiated by dialysis against inositol 1,4,5-trisphosphate (IP_3) ($40 \mu M$ IP_3 in the intrapipette solution)

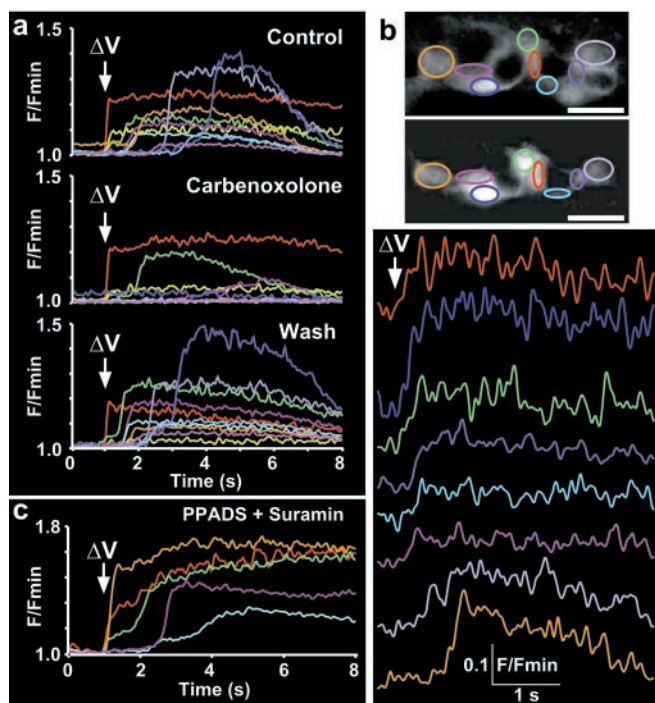


Fig. 4. Propagation of $[Ca^{2+}]_i$ waves between FS cells depends on gap junctional signaling. (a) Electrically stimulated $[Ca^{2+}]_i$ waves between FS cells (red trace: triggered cell) in normal Ringer's saline (Top) and in the presence of 100 μ M carbenoxolone (Middle) are shown. Carbenoxolone reduced the number of FS cells propagating the $[Ca^{2+}]_i$ wave in a reversible manner (Bottom). (b Top) Field of FS cells loaded with the Ca^{2+} -sensitive dye (cell circled in red: stimulated cell). (Middle) Lucifer yellow-filled cells after the patch-clamp recording of the stimulated cell (scale bar, 5 μ m). (Bottom) $[Ca^{2+}]_i$ wave triggered in response to voltage stimulation in the FS cells that subsequently showed Lucifer yellow diffusion. (c) Pyridoxal phosphate-6-azophenyl-2',4'-disulfonic acid + suramin (100 μ M each), antagonists of purinergic receptors, failed to suppress a propagated $[Ca^{2+}]_i$ wave in response to voltage stimulation.

without suppressing the initial IP_3 calcium-mobilizing response ($n = 6$ and 11 fields in control and carbenoxolone-treated cells, respectively; $P < 0.001$, χ^2 test). Interestingly, IP_3 -triggered $[Ca^{2+}]_i$ waves were much slower to propagate ($15 \pm 5 \mu\text{m/s}$, $n = 16$ cells) than electrically induced $[Ca^{2+}]_i$ waves ($P < 0.05$, Mann-Whitney U test). Finally, cell-to-cell transfer of Lucifer yellow that diffuses through most gap junctions revealed that the FS cells undergoing $[Ca^{2+}]_i$ waves were dye-coupled (Fig. 4b, $n = 7$ fields).

We then investigated the possible involvement of an extracellular route in the $[Ca^{2+}]_i$ wave propagation. Purine nucleotides have been identified as an extracellular messenger in various cells including FS cells (31), and there is evidence that they may act in concert with gap junction signaling for wave propagation in cell preparations (17–20, 22). Bath application of both pyridoxal phosphate-6-azophenyl-2',4'-disulfonic acid (PPADS) and suramin (100 μ M each), antagonists known to depress purinergic receptor transmission in glial cell networks (18), failed to suppress propagated $[Ca^{2+}]_i$ waves (Fig. 4c) ($n = 9$ fields), whereas they abolished $[Ca^{2+}]_i$ responses to ATP (10 μ M, 10-s application, $n = 23$ cells, data not shown).

FS Cell Network: A Functional Large-Scale Communication System. In the view that we imaged propagated $[Ca^{2+}]_i$ waves with a restricted spatial resolution (square fluorescent confocal images $\leq 5,600 \mu\text{m}^2$), it was important to know whether the FS cell network could transfer information over long distances within

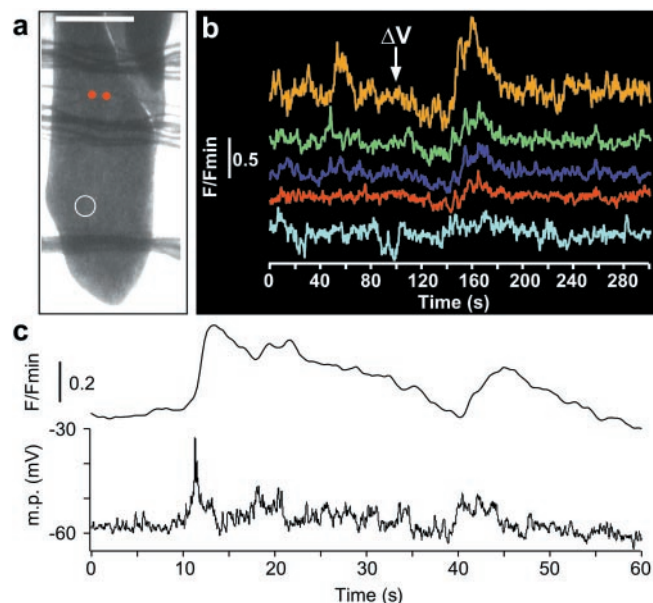


Fig. 5. Long-distance propagation of electrical and Ca^{2+} signals along the FS cell circuit. (a) Bright-field image of a coronal pituitary slice. The irregular transverse lines were the nylon threads used to keep the slice in place. The two red dots help identify the position of the two stimulation pipette tips touching the slice surface. (Scale bar, 500 μ m.) (b) $[Ca^{2+}]_i$ changes were recorded (5 frames per s) in five FS cells that were located in the region delimited by the white circle (620 μ m from the pair of stimulation pipettes) in a. Electrical stimulation (700 μ A, 75 ms) induced the occurrence of coincident $[Ca^{2+}]_i$ rises in these cells. (c) In another slice, electrical and $[Ca^{2+}]_i$ recordings were simultaneously combined in an FS cell, 520 μ m away from the point of stimulation. $[Ca^{2+}]_i$ rise did not occur, neither did depolarization between the electrical stimulation and the beginning of the plots (39-s time span). Transient depolarizing events then coincided with the propagated $[Ca^{2+}]_i$ rises.

the parenchyma. $[Ca^{2+}]_i$ imaging of FS cells combined with distant electrical field stimulation (Fig. 5a) revealed prominent, coordinated transient $[Ca^{2+}]_i$ rises that occurred far away (0.5–1 mm) from the stimulation site (Fig. 5b, 6 slices). $[Ca^{2+}]_i$ waves, which were first recruited upon electrical stimulation and then propagated along the FS cell network, were very likely to be at the origin of the distant $[Ca^{2+}]_i$ rises, as these only occurred when stimulation intensity exceeded a threshold level (700 μ A to 5 mA). Also, propagated $[Ca^{2+}]_i$ waves were closely correlated with changes in membrane potential. $[Ca^{2+}]_i$ recordings combined with patch-clamp monitoring of FS cells several hundred microns distant from the site of stimulation showed the occurrence of transient depolarization that coincided with each propagated $[Ca^{2+}]_i$ rise (Fig. 5c, $n = 5$ cells). Similar depolarizing events were detected upon propagated $[Ca^{2+}]_i$ rises in FS cells that were near single electrically stimulated FS cells ($n = 4$, data not shown). Propagated $[Ca^{2+}]_i$ rises were always associated with transient depolarization exceeding a threshold level of about -50 mV (Fig. 5c), notwithstanding the distance between the patched cells and the site of stimulation (range 17–520 μ m, $n = 9$). Inversely, such a depolarization was never observed in FS cells that failed to display propagated $[Ca^{2+}]_i$ rises ($n = 6$, data not shown).

A final set of results provided evidence that the FS cell network forms an extended three-dimensional mode of communication. Consistent with this assumption, we found that $[Ca^{2+}]_i$ waves were electrically triggered in FS cells from coronal as well as sagittal slices. Also, the apparent low velocity of $[Ca^{2+}]_i$ waves ($17.7 \pm 0.8 \mu\text{m/s}$, $n = 45$ cells, 6 fields) calculated from the distance between the pair of electrode tips and recorded FS cells (Fig. 5) suggested a complex arborization of the gap junction-

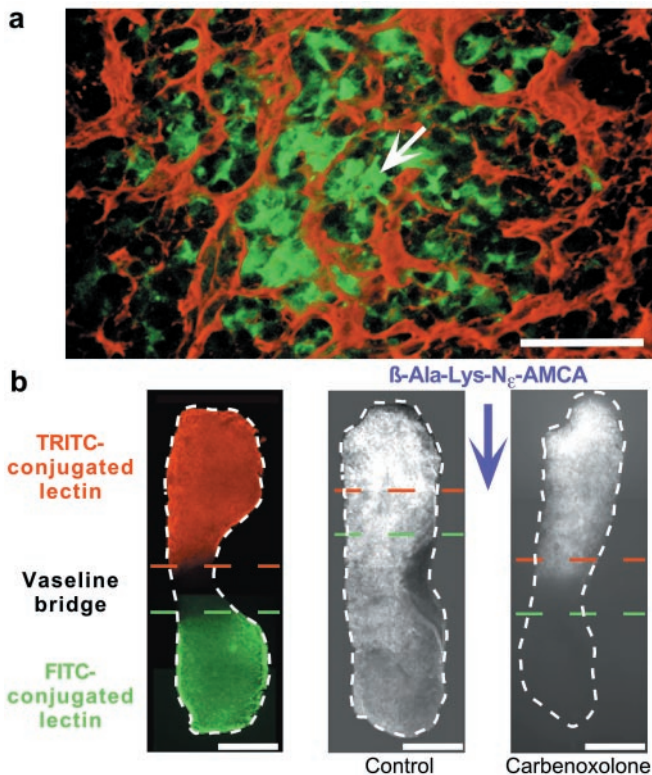


Fig. 6. Three-dimensional, large-scale communication through the FS cell network. (a) Three-dimensional reconstruction (20- μ m depth) of Neurobiotin-filled FS cells (labeled in green) together with the immunolabeling of laminin, a component of basal laminae surrounding the cell cords (labeled in red). The arrow indicates the approximate location of the cell initially recorded during 90 min with a Neurobiotin-containing patch-clamp pipette (scale bar, 50 μ m). (b) FS cell network visualized with the Vaseline-gap technique. (Left) Coronal slice straddling between two compartments of a chamber. Fluorescent lectin stainings localized the Vaseline bridge covering the slice at the compartment interface (scale bar, 500 μ m). TRITC, tetramethylrhodamine isothiocyanate. Colored dashed lines delineate the approximate location of the Vaseline bridge, whereas the white one shows the slice periphery. (Center) Bath application of β -Ala-Lys- N^{ϵ} -AMCA in the top compartment allowed the staining of FS cells across the whole slice. (Right) When carbenoxolone (100 μ M) was present in both compartments, β -Ala-Lys- N^{ϵ} -AMCA-stained FS cells were seen only in the top compartment and, marginally, within the Vaseline gap.

coupled FS cell network within the labyrinthine cell cords. Two results strengthened this proposal. First, single-cell dialysis of the Neurobiotin tracer traced a meshwork of connected FS cells over territories, which crossed cell cord boundaries (Fig. 6a, $n = 16$ fields). Second, multiple site introduction of low-molecular weight fluorescent dyes into FS cells provided further evidence for multidirectional, long-distance (millimeter range) transfer of information throughout the parenchyma (Fig. 6b). Bath application of β -Ala-Lys- N^{ϵ} -AMCA on one side of the coronal slices (insulated from the other side with a Vaseline bridge) allowed many FS cells to take up the fluorescent dipeptide. β -Ala-Lys- N^{ϵ} -AMCA diffused across the Vaseline bridge up to the opposite side of the slices ($n = 9$). Carbenoxolone (100 μ M) blocked the spreading of β -Ala-Lys- N^{ϵ} -AMCA ($n = 5$), which, given its low molecular weight (432.5) (24), probably diffused between FS cells coupled by gap junctions.

Discussion

In this study, we provide strong evidence that the anterior pituitary possesses an intrinsic system of communication that allows long-distance transfer of information within its paren-

chyma. The hitherto enigmatic agranular FS cells form the framework of this communication system. These FS cells express an extended repertoire of signaling mechanisms to generate and transmit messages (regenerative $[Ca^{2+}]_i$ waves, cell-to-cell diffusion of molecules) along their cell network wiring up the gland.

This work reveals that the FS cells can now be given the label “excitable cell,” nearly half a century after they were discovered (15). Only one study so far has shown in cultured FS cells (TtT/GF cell line) the presence of a delayed rectifier K^+ current, which was detectable when the cloned FS cells were in contact (25). We demonstrate here that, *in situ*, FS cells had a set of voltage-gated conductances sufficient to generate action potentials and ensuing transient $[Ca^{2+}]_i$ rises. To do so, FS cells displayed TTX-sensitive Na^+ currents and Cd^{2+} -sensitive Ca^{2+} currents, which both could provide a depolarization at the foot of action potential that increases the probability of spike firing. Whereas a built-in inactivation process led Na^+ channels to close quickly, the fast-activating, slow-inactivating Ca^{2+} channels apparently remained open long enough during single action potentials to cause a significant $[Ca^{2+}]_i$ increase. Also, two K^+ currents, which shared common properties with the 4-aminopyridine-sensitive I_A and TEA-sensitive delayed rectifier K^+ currents (32), respectively, helped shape the repolarizing process of action potentials.

Excitability, which may at first appear as an atypical behavior for such agranular cells, is most likely one of the means to trigger long-range $[Ca^{2+}]_i$ signaling, a hitherto unknown mode of communication at the anterior pituitary level. Brief electrical stimulation of one or a few FS cells promoted $[Ca^{2+}]_i$ waves between FS cells over long distances across the parenchyma. Because of their sensitivity to both TTX and Cd^{2+} ions, we propose that the electrical activity induced in stimulated FS cells initiated the propagation of intercellular $[Ca^{2+}]_i$ waves along the FS cell network.

A closely related question is how $[Ca^{2+}]_i$ rises traveled from one FS cell to the next. Our results strongly suggest that, *in situ*, many FS cells were extensively coupled through gap junctions and that these gap junctions were responsible for the propagation of $[Ca^{2+}]_i$ rises between the coupled cells. The involvement of gap junctions in this phenomenon was fourfold. First, the gap junction blocker carbenoxolone reversibly reduced the number of FS cells propagating $[Ca^{2+}]_i$ waves that were initiated by either focal electrical stimulation or IP_3 dialysis; second, intracellular injections of Lucifer yellow traced the FS cells that propagated $[Ca^{2+}]_i$ waves; third, intercellular diffusion of small tracers (Neurobiotin and β -Ala-Lys- N^{ϵ} -AMCA) resulted in the labeling of three-dimensional ensembles of FS cells that were also blocked by carbenoxolone; and fourth, it was highly unlikely that activation of membrane receptors, such as purinergic receptors after ATP release, be involved in $[Ca^{2+}]_i$ waves triggered after voltage stimulation.

The nature of signals flowing between gap junction-coupled FS cells that propagated electrically induced $[Ca^{2+}]_i$ waves was then addressed. Both the velocity (124 μ m/s) and extent (millimeter range) of $[Ca^{2+}]_i$ waves suggested that the latter spread along the three-dimensional FS cell network in a regenerative manner. Two types of regenerative signals seemed feasible: a cell-to-cell transfer of second messengers (22) or an electrical event (33, 34). The first possibility appeared barely compatible with our results. In FS cells, average speeds of intercellular $[Ca^{2+}]_i$ waves driven by single-cell IP_3 dialysis were slow (15 μ m/s), as has been observed for second messenger waves involving Ca^{2+} release from internal stores in a chain reaction, owing to the regenerative nature of the release process (19–22). Thus, second messenger waves could propagate between FS cells, but they were probably not representative of propagation mechanisms in most FS cells when an electrical stimulation was locally applied. In favor of the second possibility was the

detection of membrane depolarization coincident with propagated $[Ca^{2+}]_i$ rises. Such a transient depolarization probably participated in the occurrence of propagated $[Ca^{2+}]_i$ rises as it overlapped with the activation threshold of both Na^+ and Ca^{2+} channel currents. However, we did not observe large spikes that coincided with the spreading of $[Ca^{2+}]_i$ waves, possibly because of the poor space-clamp control in the highly coupled FS cells that propagated large-scale $[Ca^{2+}]_i$ waves. Consistent with this assumption, it was possible to trigger action potentials in FS cell somas, but only when the cells displayed a high input resistance. Also, the electrical signal might be filtered when passing through gap junctions, as observed between gap junction-coupled neurons (33, 34). Hence, techniques that permit subcellular monitoring of membrane potential (e.g., potential-sensitive dyes) (35) need to be developed for pituitary slices to better address this issue that should include the detection of signals within the long and slender processes of FS cells (16), which are rich in gap junctions (27).

What might be the function of such a network of cells wiring up the anterior pituitary? It has been well documented that FS cells are not just sustentacular elements but perform regulatory functions that determine the responsiveness of hormone-secreting cells (14, 29). With their long cytoplasmic processes

between other cell types, they are in an ideal position to play a role in intercellular communication mechanisms. Although FS cells do not secrete hormones, they are known to release biologically important factors and signaling molecules (e.g., IL-6, nitric oxide, vascular endothelial growth factor, basic fibroblast growth factor, follistatin) (14, 29, 36) and are responsive to central and peripheral stimuli [e.g., pituitary adenylate cyclase-activating peptide (PACAP), vasoactive intestinal peptide, estrogens] (37–39) including immune factors (tumor necrosis factor α , transforming growth factor β 3, IFN- γ) (40–42). Moreover and most remarkably, the FS cell network seems to provide a unique system of large-scale communication that may rapidly adjust cellular activities within the anterior pituitary. Hence, distant endocrine cells might receive coordinated information from both extrapituitary molecules (1–4) slowly carried by the pituitary microvasculature (5) and intrapituitary signals mostly emanating from the FS cell circuitry.

We thank A. Carrette and J.-M. Michel for technical assistance. This work was supported by Institut National de la Santé et de la Recherche Médicale and grants from the European Union, Région Languedoc-Roussillon, Association pour la Recherche sur le Cancer, and Fondation pour la Recherche Médicale.

- Knobil, E. (1980) *Recent Prog. Horm. Res.* **36**, 53–88.
- Liu, J. H., Kazer, R. R. & Rasmussen, D. D. (1987) *J. Clin. Endocrinol. Metab.* **64**, 1027–1035.
- Sassin, J. F., Frantz, A. G., Weitzman, E. D. & Kapen, S. (1972) *Science* **177**, 1205–1207.
- Plotsky, P. M. & Vale, W. (1985) *Science* **230**, 461–463.
- Porter, J. C., Ondo, J. G. & Cramer, O. M. (1974) *Handb. Physiol. Sect. Endocrinol.* **4**, 33–43.
- Baker, B. L. (1974) *Handb. Physiol. Sect. Endocrinol.* **4**, 45–80.
- Schlegel, W., Winiger, B. P., Mollard, P., Vacher, P., Wuarin, F., Zahnd, G. R., Wollheim, C. B. & Dufy, B. (1987) *Nature (London)* **329**, 719–721.
- Fomina, A. F. & Levitan, E. S. (1995) *J. Neurosci.* **15**, 4982–4991.
- Villalobos, C., Faught, W. J. & Frawley, L. S. (1998) *Mol. Endocrinol.* **12**, 87–95.
- Guérineau, N. C., Bonnefont, X., Stoeckel, L. & Mollard, P. (1998) *J. Biol. Chem.* **273**, 10389–10395.
- Bonnefont, X., Fiekers, J., Creff, A. & Mollard, P. (2000) *Endocrinology* **141**, 868–875.
- Stewart, J. K., Clifton, D. K., Koerker, D. J., Rogol, A. D., Jaffe, T. & Goodner, C. J. (1985) *Endocrinology* **116**, 1–5.
- Gambacciani, M., Liu, J. H., Swartz, W. H., Tueros, V. S., Rasmussen, D. D. & Yen, S. S. (1987) *Clin. Endocrinol.* **26**, 557–563.
- Schwartz, J. (2000) *Endocr. Rev.* **21**, 488–513.
- Rinehart, J. & Farquhar, M. (1953) *J. Histochem. Cytochem.* **1**, 93–113.
- Vila-Porcile, E. (1972) *Z. Zellforsch. Mikrosk. Anat.* **129**, 328–369.
- Guthrie, P. B., Knappenberger, J., Segal, M., Bennett, M. V., Charles, A. C. & Kater, S. B. (1999) *J. Neurosci.* **19**, 520–528.
- Scemes, E., Suadicani, S. O. & Spray, D. C. (2000) *J. Neurosci.* **20**, 1435–1445.
- Cotrina, M. L., Lin, J. H., Lopez-Garcia, J. C., Naus, C. C. & Nedergaard, M. (2000) *J. Neurosci.* **20**, 2835–2844.
- Newman, E. A. & Zahs, K. R. (1997) *Science* **275**, 844–847.
- Newman, E. A. (2001) *J. Neurosci.* **21**, 2215–2223.
- Charles, A. (1998) *Glia* **24**, 39–49.
- Garaschuk, O., Linn, J., Eilers, J. & Konnerth, A. (2000) *Nat. Neurosci.* **3**, 452–459.
- Otto, C., tom Dieck, S. & Bauer, K. (1996) *Am. J. Physiol.* **271**, C210–C217.
- Yamasaki, T., Fujita, H., Inoue, K., Fujita, T. & Yamashita, N. (1997) *Endocrinology* **138**, 4346–4350.
- Pinault, D. (1995) *Brain Res. Rev.* **21**, 42–92.
- Soji, T. & Herbert, D. C. (1989) *Anat. Rec.* **224**, 523–533.
- Yamamoto, T., Hossain, M. Z., Hertzberg, E. L., Uemura, H., Murphy, L. J. & Nagy, J. I. (1993) *Histochemistry* **100**, 53–64.
- Allaerts, W., Carmeliet, P. & Deneef, C. (1990) *Mol. Cell. Endocrinol.* **71**, 73–81.
- Alvarez-Maubecin, V., Garcia-Hernandez, F., Williams, J. T. & Van Bockstaele, E. J. (2000) *J. Neurosci.* **20**, 4091–4098.
- Chen, L., Maruyama, D., Sugiyama, M., Sakai, T., Mogi, C., Kato, M., Kurotani, R., Shirasawa, N., Takaki, A., Renner, U., et al. (2000) *Endocrinology* **141**, 3603–3610.
- Hille, B. (1992) *Ionic Channels of Excitable Membranes* (Sinauer, Sunderland, MA).
- Galarreta, M. & Hestrin, S. (1999) *Nature (London)* **402**, 72–75.
- Venance, L., Rozov, A., Blatow, M., Burnashev, N., Feldmeyer, D. & Monyer, H. (2000) *Proc. Natl. Acad. Sci. USA* **97**, 10260–10265. (First published August 15, 2000; 10.1073/pnas.160037097)
- Yuste, R., Lanni, F. & Konnerth, A. (2000) *Imaging Neurons: A Laboratory Manual* (Cold Spring Harbor Lab. Press, Plainview, NY).
- Yu, W. H., Kimura, M., Walczewska, A., Porter, J. C. & McCann, S. M. (1998) *Proc. Natl. Acad. Sci. USA* **95**, 7795–7798.
- Yada, T., Vigh, S. & Arimura, A. (1993) *Peptides* **14**, 235–239.
- Tatsuno, I., Somogyvari-Vigh, A., Mizuno, K., Gottschall, P. E., Hidaka, H. & Arimura, A. (1991) *Endocrinology* **129**, 1797–1804.
- Allen, D. L., Mitchner, N. A., Uveges, T. E., Nephew, K. P., Khan, S. & Ben-Jonathan, N. (1997) *Endocrinology* **138**, 2128–2135.
- Kobayashi, H., Fukata, J., Murakami, N., Usui, T., Ebisui, O., Muro, S., Hanaoka, I., Inoue, K., Imura, H. & Nakao, K. (1997) *Brain Res.* **758**, 45–50.
- Hentges, S., Boyadjieva, N. & Sarkar, D. K. (2000) *Endocrinology* **141**, 859–867.
- Vankelecom, H., Matthys, P. & Deneef, C. (1997) *J. Histochem. Cytochem.* **45**, 847–857.